

## 1. INTRODUCTION

The field of geometric combinatorics, and combinatorial polytopes in particular, has recently received a good deal of attention. Convex polytopes whose faces correspond to combinatorial constructions have arisen in a broad spectrum of pure and applied areas. They are tied to the structures of Hopf algebras and monoids on one side, while forming the foundation of linear programming on the other.

We have recently discovered a new “genus” of convex polytopes which both unites and extends the list of existing species. We propose three levels of new research. The first is an attack on well known open problems. These problems include specific open conjectures about relatives of the permutahedra and associahedra, as well as fundamental open questions about general polytopes. For questions about the diameters of convex polytopes our new constructions potentially provide illuminating counterexamples. In the narrower field of infinite polytope families our new examples have a reasonable chance at providing proofs of several conjectured polytope sequences.

At a second level we will prove that many of our new examples underlie algebraic structures: Hopf algebras, coalgebras and Hopf modules. Some of the polytopes just now being proven to be convex arose at first as examples of a general theorem: our research group proved that the Hopf algebraic structure can be predicted by the existence of a *graded Hopf operad* structure. The sets of vertices, of what we now know are convex polytope sequences, possess the latter structure. Now we ask whether the operad structure exists for the entire genus of polytopes we study, and whether it can always be extended to the sets of higher dimensional faces. Simultaneously we will demonstrate that their vertex sets support order structure as well—posets and lattices—and that these algebraic structures and ordered structures interact conveniently.

Finally, we will propose applications via exploiting some nice maps that we have noticed while developing our new polytopes. Several polytope families we have studied have potentially valuable interpretations: as molecular constructions (polyhexes), as phylogenetic trees, and as topological bases for networks.

At each stage we will highlight the broader impact of the project by pointing out the role student researchers will play. Master’s and undergraduate students have already been extremely active in all parts of the research. One master’s thesis and one honor’s thesis dealt with new Hopf structures on the cyclohedra. Another master’s thesis and another separate honor’s thesis gave initial results about polytopes based on CW-complexes. There are two more master’s students currently working on theses about the topics we are about to explore. Among future open questions to be assigned to students are: What are the geometrical properties of the realizations of various polytopes—centers, volumes, symmetries, edge lengths and facet areas? Also of interest are the combinatorial properties—numbers of vertices, numbers of faces, numbers of triangulations, and space tiling properties.

**1.1. What we found—poset polytopes and liftings.** For any poset  $P$  we define two combinatorial constructions that are built from special lower sets of the poset. The polytopes that result cover a wide swath of existing examples from geometric combinatorics, including the permutahedra, associahedra, multiplihedra, graph-associahedra, nestohedra, pseudograph associahedra, and their liftings.

An  $n$ -dimensional permutahedron is the convex hull of the points formed by the action of a finite reflection group on a arbitrary point in Euclidean space. The classic example is the convex hull of all permutations of the coordinates of the Euclidean point  $(1, 2, \dots, n-1)$ . Changing edge lengths while preserving their directions results in a *generalized permutohedron*, as defined by Postnikov [23, 22]. An important subclass of these is the nestohedra [29]. Nestohedra have the feature that each of their faces corresponds to a specific combinatorial set, and the intersection of two faces corresponds to the union of the two sets. For a given set  $S$  each nestohedron  $\mathcal{N}(B)$  is based upon a given *building set*  $B \subset \mathcal{P}(S)$ , whose elements are known as tubes.  $B$  must contain all the singletons of  $S$  and must also contain the union of any two tubes whose intersection is non-empty. Then a face of the nestohedron corresponds to a *nested set*  $F$ .  $F$  is a subset of  $B$  for which each pair of tubes is *compatible* (either one is contained in the other or their union is not in  $B$ ) and for which any collection of disjoint tubes must not have a union in  $B$ .

Our first new family of convex polytope are a generalization of nestohedra via a generalization of building sets. Rather than starting with a set  $S$  we begin with a poset  $P$ . For a subset  $A$  of poset  $P$ , define the *lower set* of  $A$  as  $\tau_A := \{b \in P \mid b \leq a \text{ for some } a \in A\}$ . A lower set with unique maximal element  $a$  is called a *cell*  $\tau_a$ , having *boundary*  $\partial\tau_a := \tau_a - a$ .

**Definition 1.1.** Let  $\mathbf{b}_a := \{b \in P \mid \partial\tau_a = \partial\tau_b\}$  be the bundle of the cell  $\tau_a$ . A lower set is filled if, whenever it contains the boundary  $\partial\tau_a$  of a cell, it also intersects the bundle  $\mathbf{b}_a$  of that cell.

**Definition 1.2.** Definition. A tube is a filled, connected lower set. A tubing  $T$  is a collection of tubes (not containing all of  $P$ ) which are pairwise disjoint or pairwise nested, and for which the union of every subset of  $T$  is filled.

Examples of tubes and tubings are seen in Figure 1.

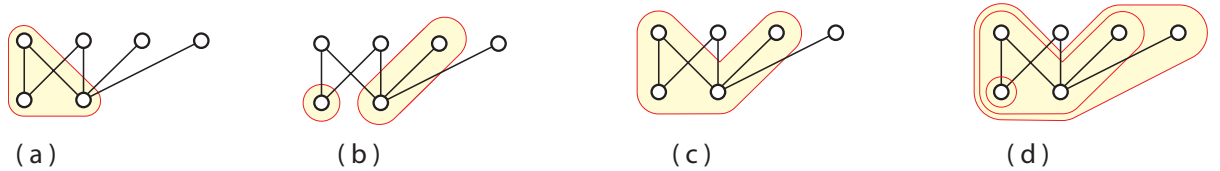


FIGURE 1. Here is a Hasse diagram of a poset with various lower sets circled. (a) and (b) are not valid tubings, since both fail to be filled. (c) and (d) are tubings.

**Theorem 1.3.** . Let  $P$  be a poset, where  $B = \{\mathbf{b}_1, \dots, \mathbf{b}_k\}$  is the set of bundles of  $P$ . Let  $\pi(P)$  be the poset of tubings of  $P$  ordered by containment. The poset associahedron  $KP$  is a convex polytope of dimension  $|P| - k$  whose face poset is isomorphic to  $\pi(P)$ .

We believe we have a nice inductive proof of this main theorem, which should be published soon. Induction is on the number of elements in the poset: as a new maximal element is added

new facets are added to the polytope depending on which lower sets are now tubes. Figures 2, 3 and 4 show some examples.

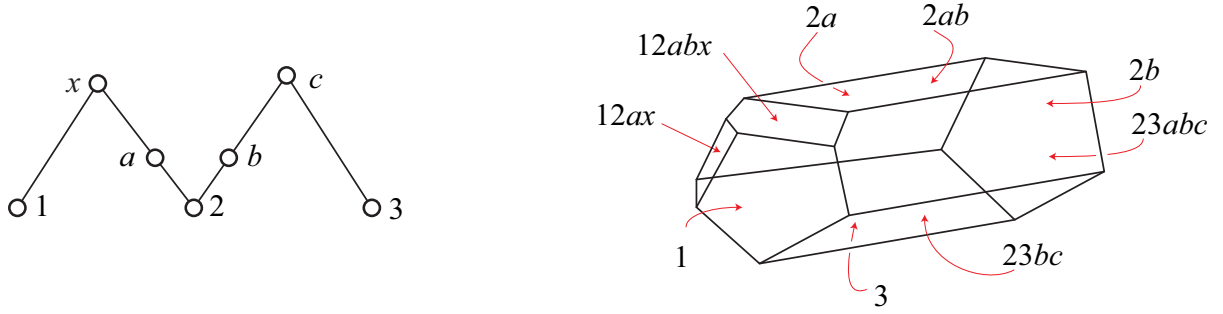


FIGURE 2. On the left is a poset, shown as a Hasse diagram. On the right is its poset associahedron, with labeled facets corresponding to tubes of the poset.

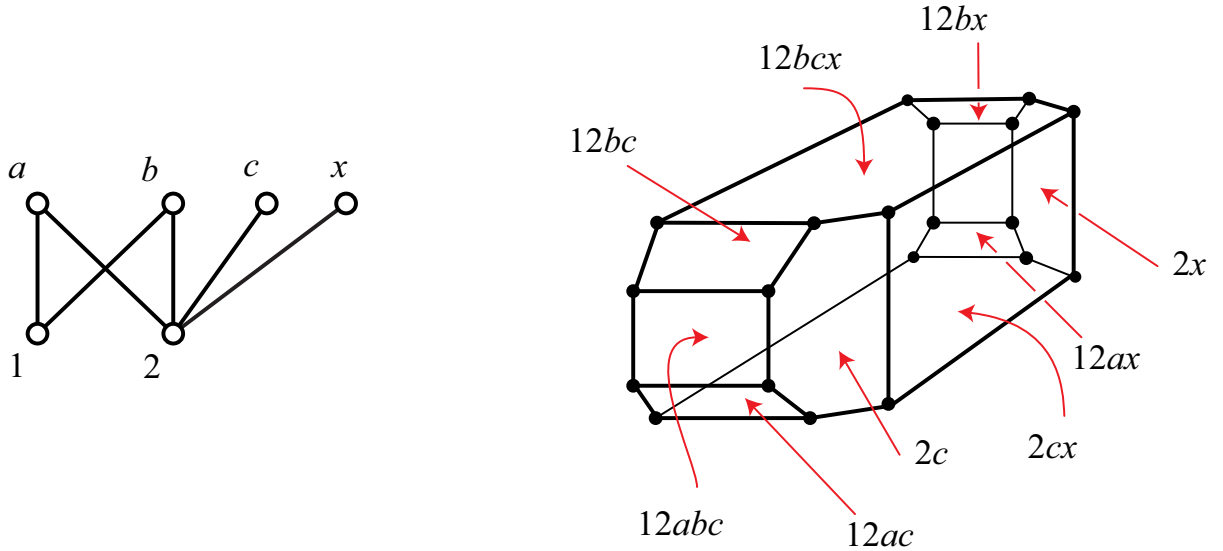


FIGURE 3. On the left is another poset. On the right is its poset associahedron, with labeled facets again corresponding to tubes of the poset.

The poset polytopes we have introduced cover many of the known varieties of simple polytopes: permutohedra, associahedra, graph-associahedra, nestohedra and pseudograph-associahedra, as seen in [5], all correspond to certain sub-classes of posets. In fact, all these types are from rank two posets. Nestohedra come from posets of rank two with all bundles of size one. Pseudograph-associahedra come from posets of rank two with only one or two minimal rank elements covered by each maximal element. Newly discovered are the CW-complex associahedra. Example graphs, pseudographs, CW-complexes and building sets are shown together with their posets in Figure 5, and with tubes in Figure 6. (We even have some examples of V. Pilaud's brick polytopes that fit into the poset polytope picture [21]. Determining whether all brick polytopes are poset polytopes, or vice versa, might be a crucial step in the first stage of our research program.)

**1.2. CW-complex associahedra.** When the poset  $P$  is the face poset of a cell complex, then the poset associahedron is labeled by sub-complexes.

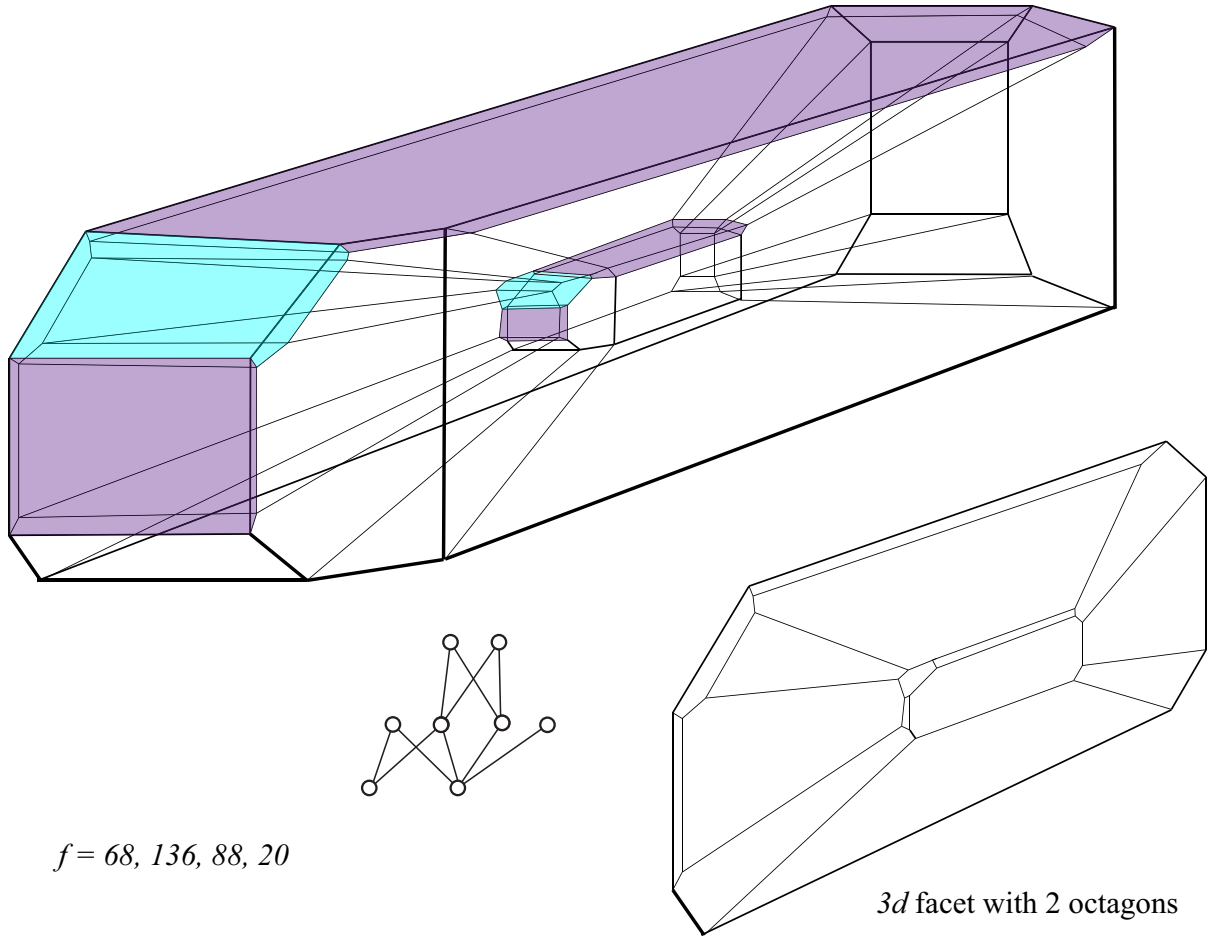


FIGURE 4. Here is a 4d example. The poset associahedron is shown above the poset it comes from. The f-vector is given, and one of the facets is shown. This example is likely a polytope that is completely new; it appears neither as a nestohedron nor a pseudograph associahedron.

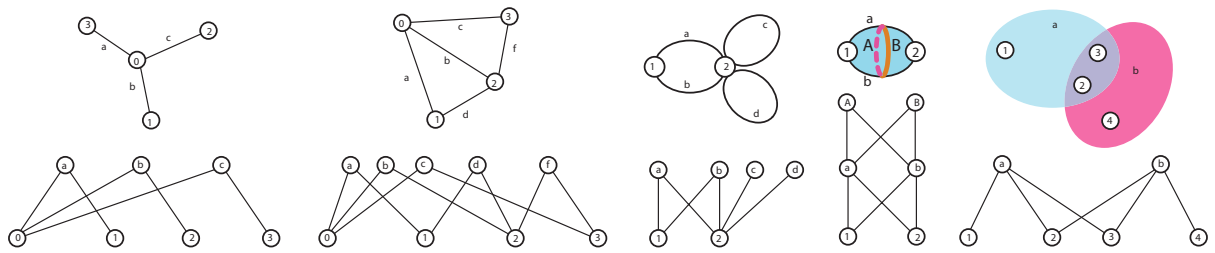


FIGURE 5. Various posets whose tubings give famous combinatorial polytopes. Left to right: star graph, fan graph, pseudograph, CW-complex (the capital letters are 2-cells) and a building set (certain kind of hypergraph).

**Example 1.4.** Let  $X$  be the cell complex with two 2-cells (labeled  $A$  and  $B$ ), two 1-cells (labeled  $a$  and  $b$ ), and two 0-cells (labeled  $1$  and  $2$ ); where  $\partial A = \partial B = a \cup b \cup 1 \cup 2$  and  $\partial a = \partial b = 1 \cup 2$ . The tubes of  $X$  are:  $1, 2, 12a, 12b, 12abA, 12abB$ . Each tube is compatible with every tube that has a different number of cells in it, and  $KX$  is the 3-dimensional cube. See Figure 7.

**Example 1.5.** Let  $X$  be the cell complex with two 2-cells (labeled  $A$  and  $B$ ), three 1-cells (labeled  $a, b$ , and  $c$ ), and two 0-cells (labeled  $1, 2$ , and  $3$ ); where  $\partial A = \partial B = a \cup b \cup c \cup 1 \cup 2 \cup 3$  and



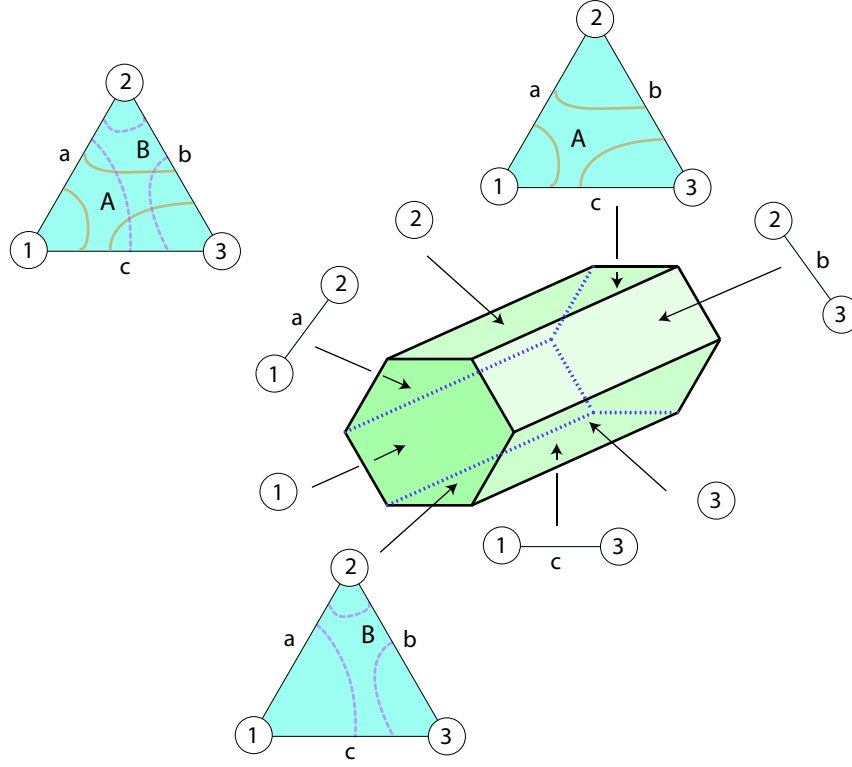


FIGURE 8. The hexagonal prism as a cellohedron.

the polynomials which give volumes of the new polytopes. Another question, that they do not address, is whether the range quotients of the lifted polytopes are themselves generalized permutohedra. These are also known as the cubeahedra in [10], and are simple polytopes—whereas the multiplihedra and their domain quotients are often non-simple.

Combinatorially, lifting occurs when the notion of a tube is extended to include markings.

**Definition 1.6.** A marked tube of  $P$  is a tube with one of three possible markings:

- (1) a thin tube  $\bigcirc$  given by a solid line,
- (2) a thick tube  $\bigotimes$  given by a double line, and
- (3) a broken tube  $\bigodot$  given by fragmented pieces.

Marked tubes  $u$  and  $v$  are compatible if

- (1) they form a tubing and
- (2) if  $u \subset v$  where  $v$  is not thick, then  $u$  must be thin.

A marked tubing of  $P$  is a tubing of pairwise compatible marked tubes of  $P$ . Examples of marked tubes are seen in Figure 9.

Although the original poset associahedron is a simple polytope its lifting is not in general simple. The proof that this always gives a convex polytope will be a little more difficult, but should follow the examples of special cases shown so far. In 2004 it was discovered by J.L. Loday that a simple algorithm existed for finding the actual points in space that are the vertices of the associahedron [18]. This algorithm was generalized to the multiplihedra and composihedra by the P.I. in [11], and to the graph-multiplihedra and their range and domain quotients in [8].

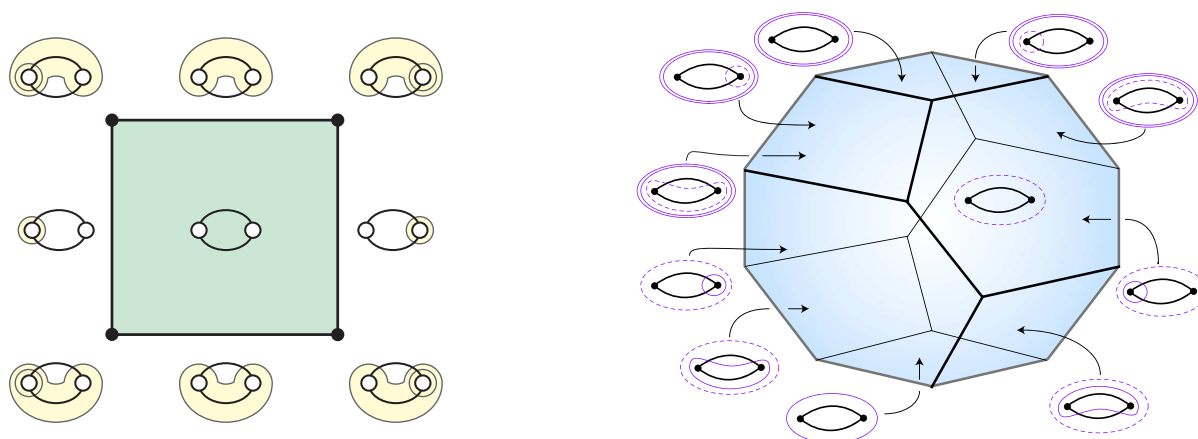


FIGURE 9. On the left is the polytope labeled by tubings of the pseudograph, and on the right is its lifting, labeled by marked tubings.

## 2. PROBLEM SOLVING I: PROVING CONJECTURED SEQUENCES OF CONVEX POLYTOPES.

The first stage of research beyond investigating and classifying the poset polytopes themselves is to try and use them to prove several conjectures. The conjectures are: that the complex of multitrangulations of a polygon form convex polytopes, that the complexes of leveled trees grafted to binary trees or leveled trees form convex polytopes, and that the complex of ordered forests of leveled trees form convex polytopes. For each of these conjectures our approach is to find posets whose polytopes, or their liftings, are isomorphic (as posets) to the complex in question. We have high hopes that this attack is likely to succeed, because it has already in several similar cases.

We'll begin with the grafted, or painted, trees—since this is where we have some definite success. Three types of planar rooted trees are well known to underlie three infinite families: leveled trees underlie the permutohedra, binary trees underlie the associahedra and combed trees (also drawn as corollas) have only one representative for each number of leaves, so they underlie the natural numbers. Grafting a pair of these types of trees together, while retaining their distinguishing characteristics, is described nicely by the composition of species in [12]. Figure 10 shows the possible ways to graft two of these types of trees. We immediately wonder whether the grafted combinatorics leads to a new polytope family in each case. Figure 11 shows that we do in dimension 3, and that we know several cases in all dimensions.

Recently (in unpublished work with M. Ronco and our students) we were able to show that the complex of binary trees grafted to leveled trees, and the complex of combed trees grafted to leveled trees, are both isomorphic to certain poset polytopes. The posets in question are those for the fan graphs and the star graphs, as seen in Figure 5. This result answers the two open questions, and also suggests a new area of research in Hopf algebras (see Section 3.4. The latter is due to the fact that the complexes of grafted trees were originally introduced as Hopf algebras—now our bijection shows how to multiply and comultiply in the world of tubes and tubings. More information may soon flow both ways: new geometric realizations of the grafted tree complexes may provide new realizations of graph-associahedra.

Figure 12 shows the correspondence, exemplified in dimension 3, between the combed trees grafted to leveled trees and tubings of the star graph. Figure 13 shows the correspondence, exemplified in dimension 3, between the binary trees grafted to leveled trees and tubings of the

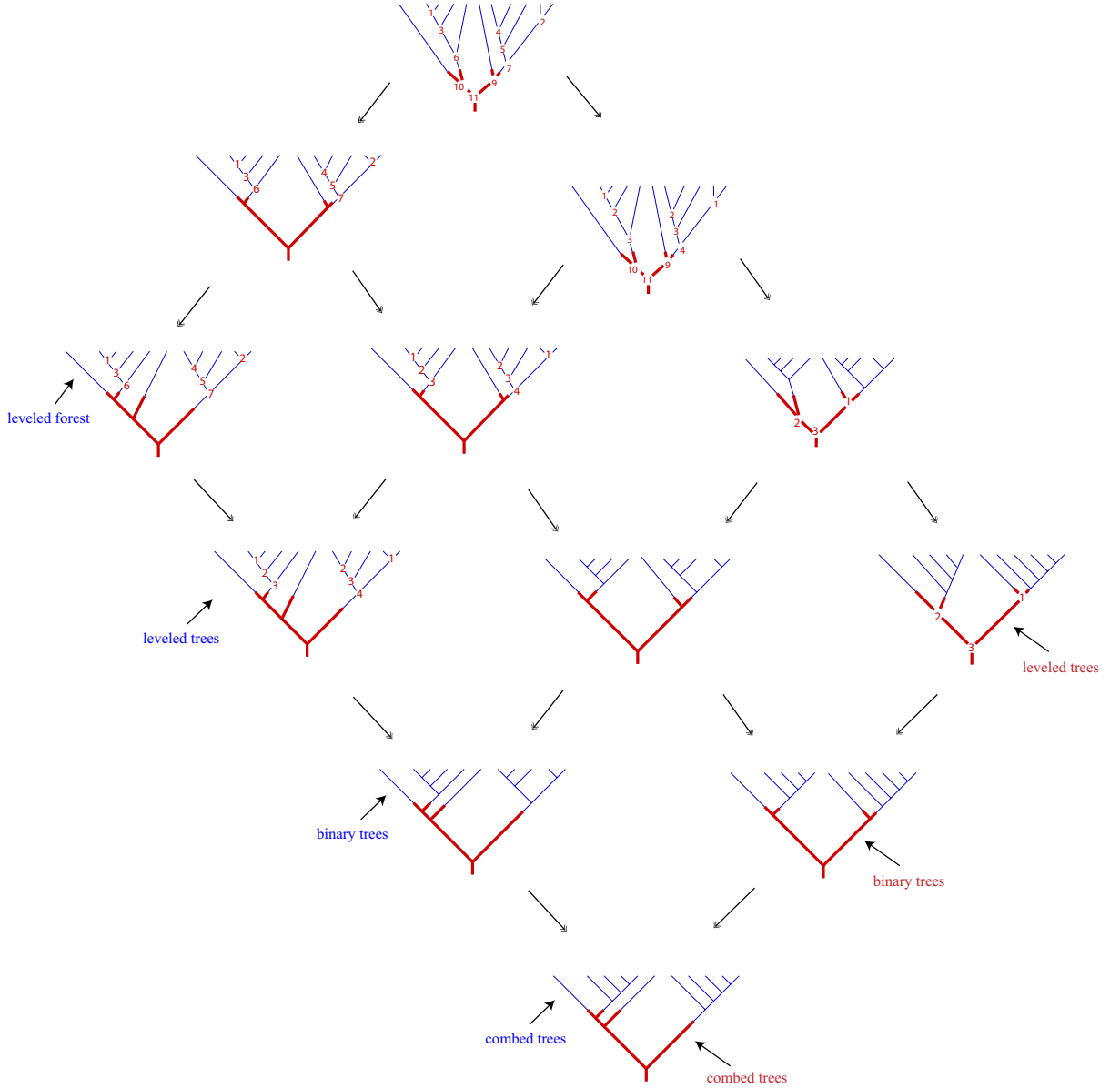


FIGURE 10. Varieties of grafted, hybrid trees. Each diagonal shares a type of tree on the bottom (shaded) or a type of tree grafted on, as indicated by the labels. These are the vertex labels of the polytopes shown in Figure 11.

fan graph. We omit for brevity all but the demonstration of the bijection for the vertices, but it is not hard to extend it to all the faces of the respective polytopes.

This combinatorial equivalence we recently discovered shows that the Hopf algebra (described in [12] and coming up next in this proposal) is both based on the vertices of convex polytopes and is nicely represented by operations on star-graph tubings.

Of course we plan to look for similar bijections that can settle the question of convexity for the conjectured polytope sequences in Figure 11.

**2.1. Plans for more–multiassociahedra, species composition, biassociahedra.** A multitriangulation of a polygon is a set of diagonal edges connecting pairs of vertices. Specifically a  $k$ -triangulation of an  $n$ -gon is a set of diagonals such that no more than  $k$  of the edges are mutually crossing. For a given value of  $n$  ordering the  $k$ -triangulations by inclusion of edges



gives a simplicial, spherical complex. Thus its polar is potentially a simple polytope, but this

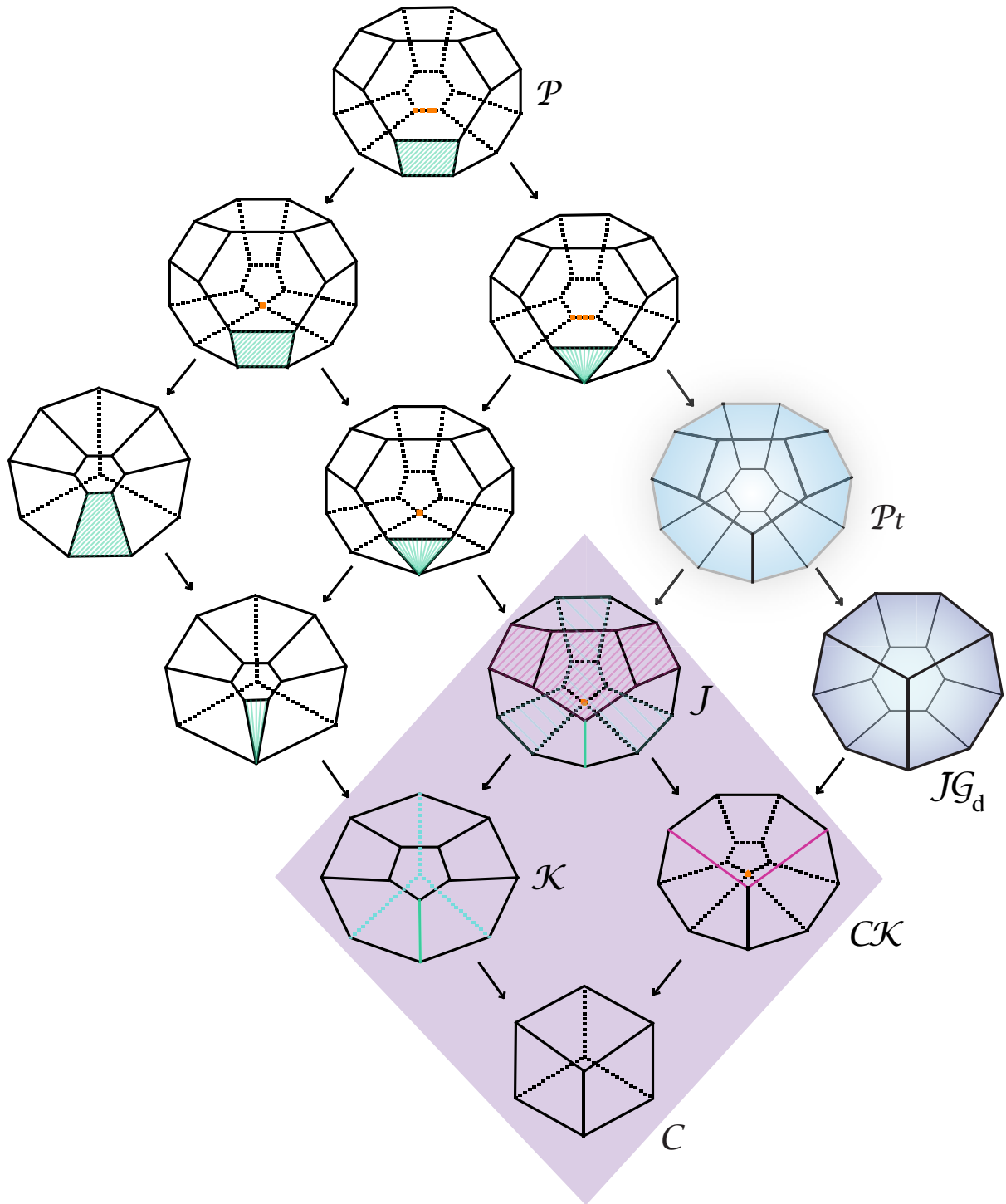


FIGURE 11. the 3d terms of some new and old polytope sequences. The four in the shaded diamond are the cube, associahedron  $\mathcal{K}$ , multiplihedron  $\mathcal{J}$  and composihedron  $\mathcal{CK}$ . The other two shaded are the pterahedron  $\mathcal{P}_t$  (fan graph associahedron) and the stellahedron  $\mathcal{JG}_d$ . The topmost is the permutohedron and the others are conjectured to be polytopes (clearly they are in three dimensions—the conjecture is about all dimensions.) Each of these corresponds the type of tree shown in Figure 10, in the corresponding position.

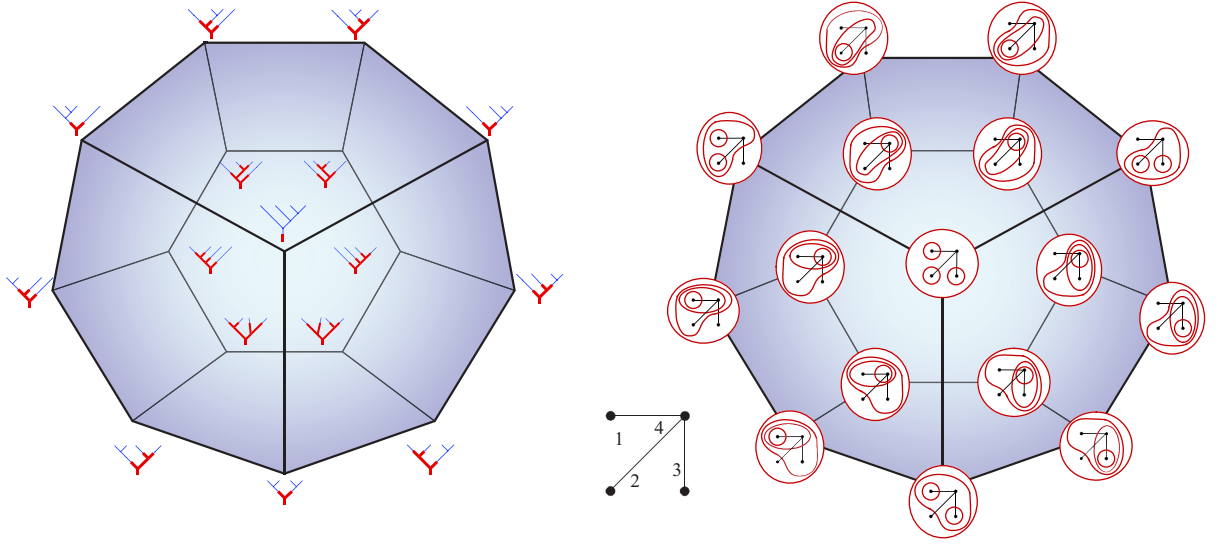


FIGURE 12. Two pictures of the stellohedron in 3d: trees and graph tubings.

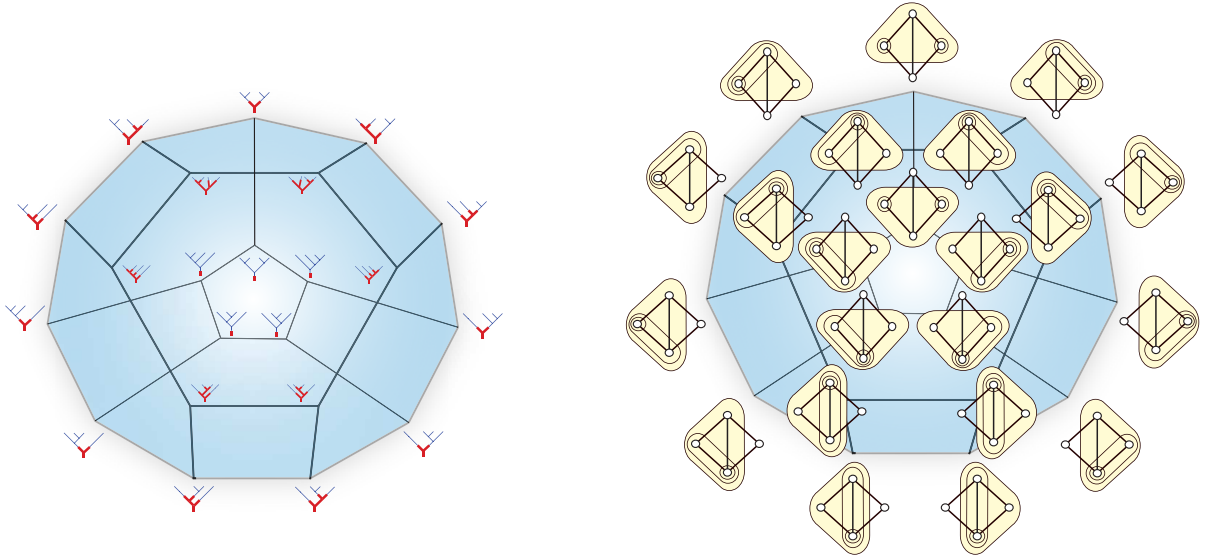


FIGURE 13. Two pictures of the pterahedron in 3d: trees and graph tubings.

has only been proven in special cases. 1-triangulations give the famous associahedra, and  $k$ -triangulations of the  $(2k + 3)$ -gon correspond to the cyclic polytopes with  $2k + 3$  vertices in dimension  $2k$ .

We plan to find specific posets whose associated simple polytopes are the (polars of) multi-associahedra. We know which posets correspond to the 1-triangulations of polygons and thus the associahedra: these are the rank two posets which realize the inclusion of nodes in edges of the path graph. An obvious first choice for the multiassociahedra is the path graph with multiedges. We also are looking for the cyclic polytopes with  $2k + 3$  vertices in dimension  $2k$ , realized as poset polytopes.

Two more conjectured varieties of convex polytope sequence we plan to try to find as poset associahedra or their liftings are 1) biassociahedra and bimultiplihedra as seen in [27], and 2)

pairahedra as seen in [28] (in the case of pairahedra there is some doubt as to whether the conjecture has been solved.)

The lifting of the permutahedron is again the permutahedron, one dimension higher. This is restated as the fact that the graph multiplihedron of the complete graph is the permutahedron. A new set of quotient polytopes arises from the deletion of the edges of the complete graph, and the forgetting of thick and thin structure. This can proceed as a two-stage process, equating the tubings that originally differed only within thick tubes, and then equating the tubings that differed only in thin tubes. Or we could factor in the other order. For an example of the two options see the top four maps of Figure 14. Of course the plan is for students to study the algebraic structure of these new polytopes.

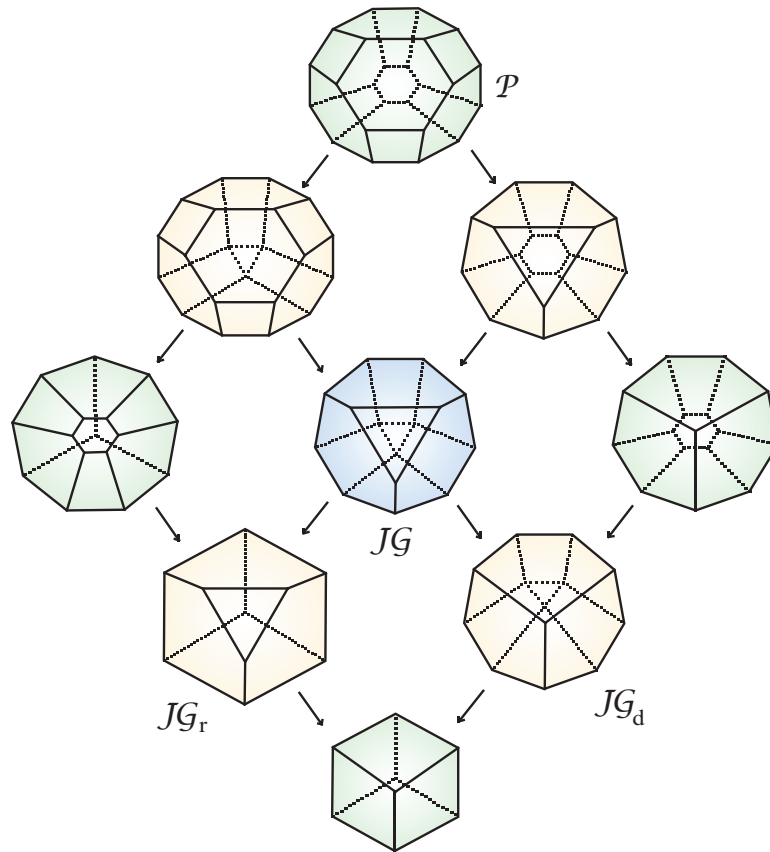


FIGURE 14. The commuting diamond of polytopes for  $G$  the edgeless graph on three nodes.

### 3. APPLICATIONS

**3.1. Hopf algebras.** A combinatorial sequence that is created by a recursive process often carries the seed of a graded algebraic structure. An algebra reflects the process of building a new object from prior ones; and a coalgebra arises from de-constructing an object into its constituent components. We are building upon the foundations laid by many other researchers, especially Gian-Carlo Rota, who most clearly saw the strength of this approach. This proposal will transition between new polytopes, newly defined operadic structure, and the newly discovered algebras. At each stage we will highlight the broader impact of the project by pointing out the role student researchers will play.

**3.2. Review of important Hopf algebras based on trees.** The historical examples of Hopf algebras  $\mathfrak{S}Sym$  and  $\mathcal{Q}Sym$ , the Malvenuto-Reutenauer Hopf algebra and the quasisymmetric functions, can be defined using graded bases of permutations and boolean subsets respectively. Loday and Ronco used the fact that certain binary trees can represent both sorts of combinatorial objects to discover an intriguing new Hopf algebra of planar binary trees,  $\mathcal{Y}Sym$ , lying between them. [18, 19]. They also described natural Hopf algebra maps which neatly factor the descent map from permutations to boolean subsets. Their first factor turns out to be the restriction (to vertices) of the Tonks projection from the permutohedron to the associahedron. Chapoton made sense of this latter fact when he found larger Hopf algebras based on the faces of the respective polytopes [7].

Much more of the structure of these algebras has been uncovered in the last decade. In 2005 and 2006 Aguiar and Sottile used alternate bases for the Loday-Ronco Hopf algebra and its dual to construct explicit formulas for primitive elements [3],[2]. Several descriptions of the big picture of combinatorial Hopf algebras have put these structures in perspective, notably [1], and [14], and most recently the preprint of Loday and Ronco [17].

**3.3. New insights into  $\mathfrak{S}Sym$ ,  $\mathcal{Y}Sym$  and divided powers.** In our recent paper [13] we take the novel point of view of graph associahedra from which to study these algebras. First we show how the Hopf algebras  $\mathfrak{S}Sym$  and  $\mathcal{Y}Sym$  and the face algebras  $\mathfrak{S}\tilde{S}ym$  and  $\mathcal{Y}\tilde{S}ym$  containing them can be understood in a unified geometrical way, via cellular surjections and recursive facet inclusion. For an example of the product of basis elements of  $\mathfrak{S}Sym$ , see Figure 15. Then we capitalize on that unified viewpoint to build analogous algebraic structures on the vertices and faces of the cyclohedra and simplices, which we describe below in Section 3.7.

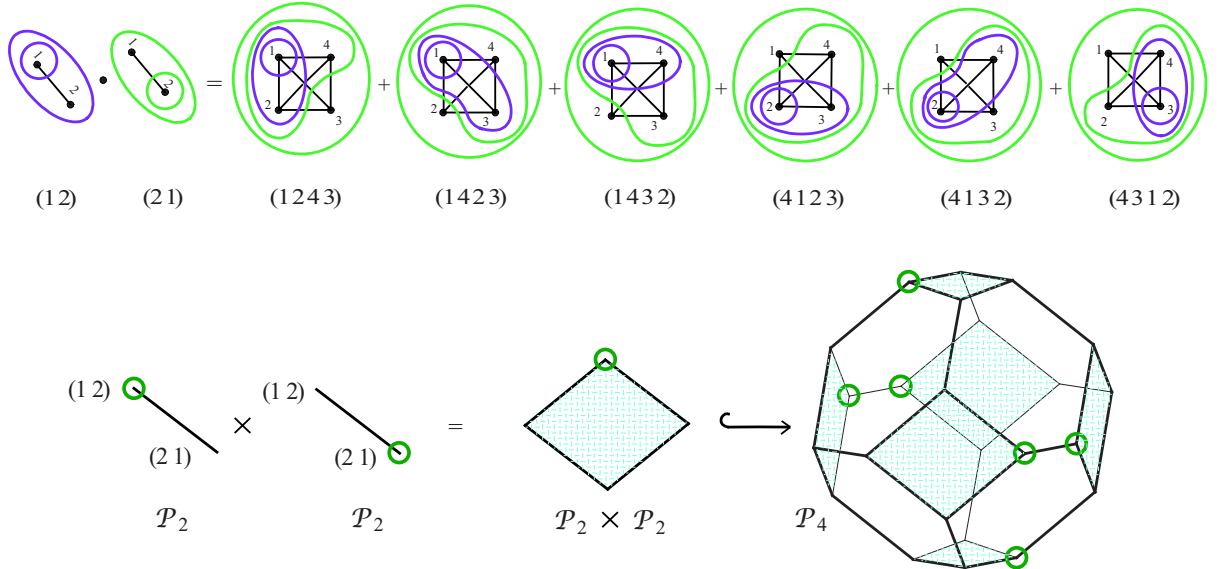


FIGURE 15. Multiplying in  $\mathfrak{S}Sym$ . The theme of [13] is that the product of two faces from a given recursive sequence of polytopes, here from terms  $\mathcal{P}_i$  and  $\mathcal{P}_j$  of the permutohedra, is described as a sum of faces of the term  $\mathcal{P}_{i+j}$ . The summed faces in the product are the images of maps which embed a cartesian product of the earlier terms of  $\{\mathcal{P}_n\}$ .

Now, in [12], we introduce a new characterization of  $\mathfrak{S}Sym, \mathcal{Y}Sym$  and the divided power Hopf algebra. The latter is denoted  $\mathcal{K}[x] := \text{span}\{x^{(n)} : n \geq 0\}$ , with basis vectors  $x^{(n)}$  satisfying  $x^{(m)} \cdot x^{(n)} = \binom{m+n}{n} x^{(m+n)}$ ,  $1 = x^{(0)}$ ,  $\Delta(x^{(n)}) = \sum_{i+j=n} x^{(i)} \otimes x^{(j)}$ .

Our new point of view sees all three of these as *graded Hopf operads*, which are graded monoids in the category of coalgebras, with the monoidal structure given by the composition product. In other words, they are simultaneously operads and coalgebras using the same grading, and with operad compositions required to be coalgebra morphisms. This implies their Hopf algebra structure. The coproduct is already given and the product is via first applying the coproduct  $n$  times to the first operand, where  $n$  is the rank of the second operand. Then the composition of the operad is applied. In terms of trees, the first operand is split into a forests of  $n$  trees, and then these are grafted to the leaves of the second operand.

**3.4. New Hopf structures on painted trees.** In [12] we show how new coalgebras are formed by composing pairs of old ones. Then we prove new Hopf algebra structures, based on operad compositions and operad actions, for the diamond of nine tree types found by excluding the upper left diagonal in Figure 10. Here for example is the new product, demonstrated on composition trees (using corollas rather than combed trees) which are at the bottom of the diamond.

$$F_{13} \bullet F_2 = \begin{array}{c} \text{Tree 1} \end{array} \bullet \begin{array}{c} \text{Tree 2} \end{array} = \begin{array}{c} \text{Tree 3} \end{array} + \begin{array}{c} \text{Tree 4} \end{array} + \begin{array}{c} \text{Tree 5} \end{array} + \begin{array}{c} \text{Tree 6} \end{array}$$

$$F_{113} + F_{113} + F_{122} + F_{131}$$

The coproduct is the usual splitting of trees:

$$\Delta F_{13} = \begin{array}{c} \text{Tree 1} \end{array} = \begin{array}{c} \text{Tree 2} \end{array} \otimes \begin{array}{c} \text{Tree 3} \end{array} + \begin{array}{c} \text{Tree 4} \end{array} \otimes \begin{array}{c} \text{Tree 5} \end{array} + \begin{array}{c} \text{Tree 6} \end{array} \otimes \begin{array}{c} \text{Tree 7} \end{array} + \begin{array}{c} \text{Tree 8} \end{array} \otimes \begin{array}{c} \text{Tree 9} \end{array}$$

$$= F_1 \otimes F_{13} + F_{11} \otimes F_3 + F_{12} \otimes F_2 + F_{13} \otimes F_1$$

Next we plan to attack the problems of finding formulas for the primitives and antipodes of some of these algebras. The bijections that prove the two conjectures (by showing combinatorial equivalence to the stellahedra and pterahedra) also allow us to describe the products and coproducts using graph tubings. These descriptions are a good deal simpler than the original descriptions using trees, so there is reason to believe that they will facilitate the finding of formulas for the antipodes and for primitive elements.

The connection between the algebra and order theory is also interesting: the 1-skeleton of our polytopes conjecturally always realizes relations of a lattice, often it is indeed the Hasse diagram of a famous lattice—the Tamari lattice, the Bruhat lattice and the Cambrian lattices of Reading all being examples seen in the well-known families of polytopes. Chains, intervals and antichains in these lattices are important. Specifically the Mobius tranformation with respect to this lattice yields easy proofs of formulas for primitive elements in the associated Hopf algebras: [3],[2]. With that in mind we plan to spend some time studying the partial orders that naturally occur on the vertex sets of our new polytopes, starting with the graphs.

**3.5. New orders on tubings.** The question might be asked: how easily may the weak order on permutations and the Tamari order be generalized to  $n$ -tubings on a graph with nodes numbered  $1, \dots, n$ ? In order to describe the ordering we give the covering relations. We can use the same notation as when comparing tubings in the poset of faces of the graph associahedron since in that poset the  $n$ -tubings are not comparable.

**Definition 3.1.** *Two  $n$ -tubings  $T, T'$  are in a covering relation  $T' \prec T$  if they have all the same tubes except for one differing pair. We actually compare the outermost nodes, one from each of the pair of differing tubes. The outermost node of a tube is the node that is included in no other smaller sub-tube of the tubing. If the number of that node is greater for  $T$ , then  $T$  covers  $T'$ .*

Note that each such covering relation corresponds to a unique  $(n-1)$ -tubing: the one resulting from removing the differing tubes. Thus the covering relations correspond to the edges of the graph associahedron.

For example, in Figure 16 we show a covering relation between two tubings on the complete graph on four numbered nodes. This figure also demonstrates the bijection between  $n$ -tubings and permutations of  $[n]$ . The nodes are the inputs for the permutation, and the output is the relative tube size. E.g., in the left-hand permutation the image of 2 is 1, and so we put the smallest tube around 2. To see the relation via tubes, we write down the sets of nodes in each tube. Only one pair of tubes differs. We compare the two numbered nodes of these which are in no smaller tubes. Here  $(3124) \prec (4123)$  since  $1 < 4$ .

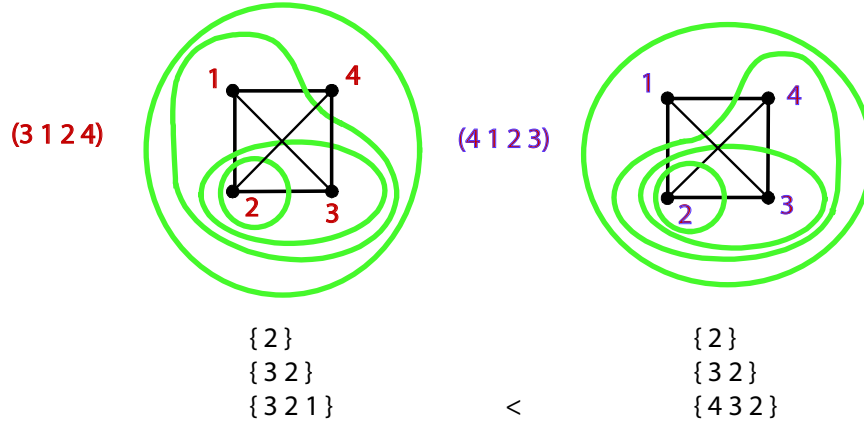


FIGURE 16. A covering relation in the weak order on permutations.

It turns out that the relation generated by these covering relations of tubings has been independently demonstrated to be a poset by Ronco [26]. In her article, the poset we have described on  $n$ -tubings of a graph is seen as the restriction of a larger poset on all the tubings of a graph.

Figure 17 shows the lattice that results from the cycle graph, recovering the cyclohedron in dimension 3. The Hasse diagram is combinatorially equivalent to the 1-skeleton of the cyclohedron. Notice that this is quite different from the type  $B_3$  Cambrian lattice described by Reading in this volume [25], despite the fact that the latter also is combinatorially equivalent to the 1-skeleton of the cyclohedron. Figure 18 shows the corresponding lattice on 4-tubings of

the star graph on 4 nodes. This Hasse diagram is combinatorially equivalent to the 1-skeleton of the 3d stellohedron. Figure 19 shows both the cyclohedron and stellohedron lattices again, unlabeled, with a different view of each polytope for comparison.

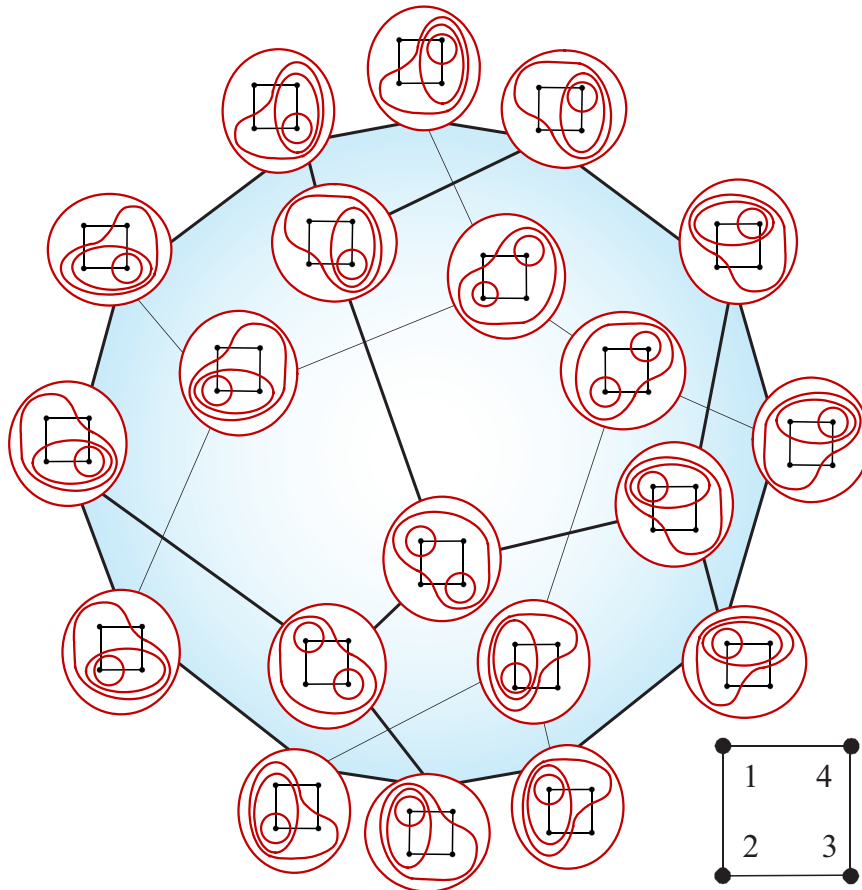


FIGURE 17. This Hasse diagram is labeled by tubings of the cycle graph, with nodes numbered 1–4. The covering relations are also a picture of the edges of the cyclohedron.

We note that as seen in Ronco’s article [26], the Tamari lattice is found as the lattice of  $n$ -tubings on the path graph with nodes numbered  $1, \dots, n$  in the order that they are connected by edges. Several open questions present themselves: for one, we notice that the 3-dimensional graph associahedra pictured here have associated posets which upon inspection prove to be lattices—it is not clear that they always are.

**3.6. Graph associahedra and cellular projections.** In [6] and [9] Carr and Devadoss show that for every graph  $G$  there is a unique convex polytope  $\mathcal{K}_G$  whose facets correspond to connected induced subgraphs. The P.I. first suspected the existence of new algebras based on  $\mathcal{K}_G$  after his discovery (published in [13]) that the Tonks projection from the permutohedron to the associahedron can be factored through a series of graph-associahedra. This fact is simple to demonstrate; it follows from Devadoss’s discovery that the complete graph-associahedron is the permutohedron while the path graph-associahedron is the Stasheff polytope. Thus by deleting edges of the complete graph one at a time, we describe a family of quotient cellular projections. Figure 20 shows one of these.

Our important result is that the cellular projections give rise to graded algebra maps.



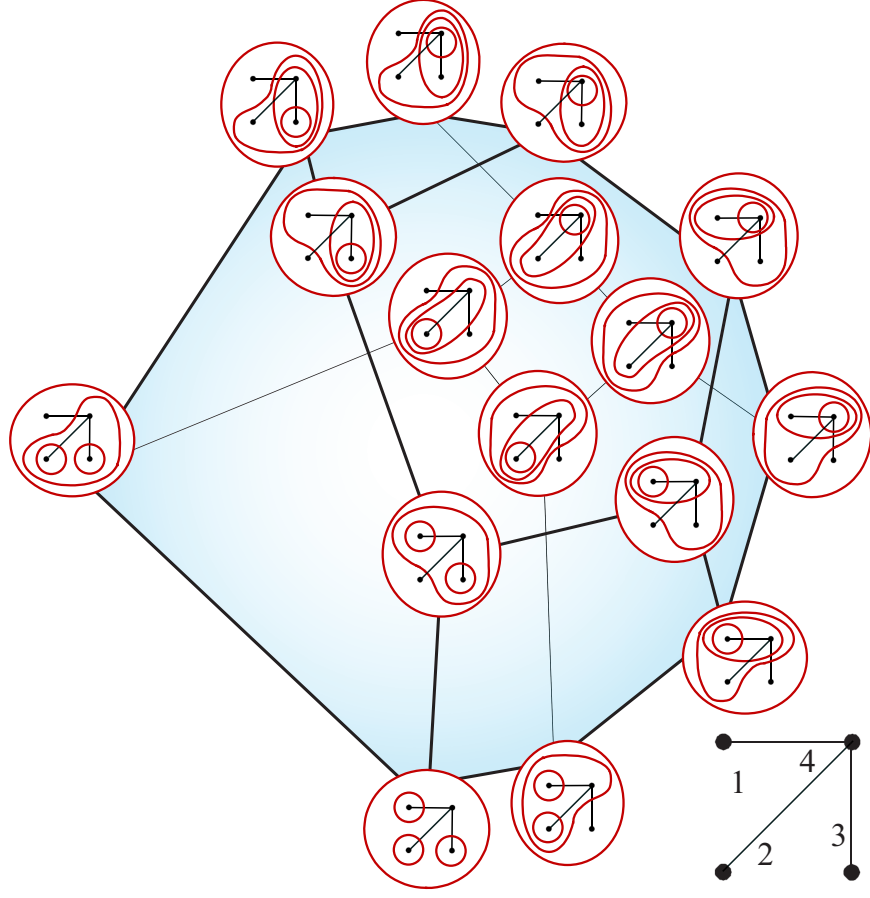


FIGURE 18. This Hasse diagram is labeled by tubings of the star graph, with nodes numbered 1–4. The covering relations are also a picture of the edges of the stellohedron.

**3.7. New algebras and modules: cyclohedron and simplex.** In our recent paper [13] we demonstrate associative graded algebra structures on the vertices of the cyclohedra and simplices, denoted  $\mathcal{WSym}$  and  $\Delta Sym$ . We also extend this structure to the full poset of faces. Figure 21 shows the product of a pair of vertices in the cyclohedron.

The number of faces of the  $n$ -simplex, including the null face and the  $n$ -dimensional face, is  $2^n$ . By adjoining the null face here we thus have a graded algebra with  $n^{th}$  component of dimension  $2^n$ . A fascinating convergence now appears.

**Theorem 3.2.** *The Hopf algebra of simplex faces  $\Delta \tilde{Sym}$  is isomorphic to the algebraic opposite of the algebra of compositions with the painted tree product.*

The proof of this theorem is in [12]. Here is an example; compare this with the example in section 3.4 by using the bijection between subsets  $\{a, b, \dots, c\} \subset [n]$  and compositions  $(a, b - a, \dots, n + 1 - c)$  of  $n + 1$ .

$$\begin{aligned}
 F_{\emptyset} \cdot F_{\{1\}} &= \\
 \text{(green circle)} \cdot \text{(red circle)} &= \text{(green circle, red circle)} + \text{(red circle, green circle)} + \text{(green circle, green circle)} + \text{(red circle, red circle)} \\
 &= F_{\{1,2\}} + F_{\{1,2\}} + F_{\{1,3\}} + F_{\{1,4\}}
 \end{aligned}$$



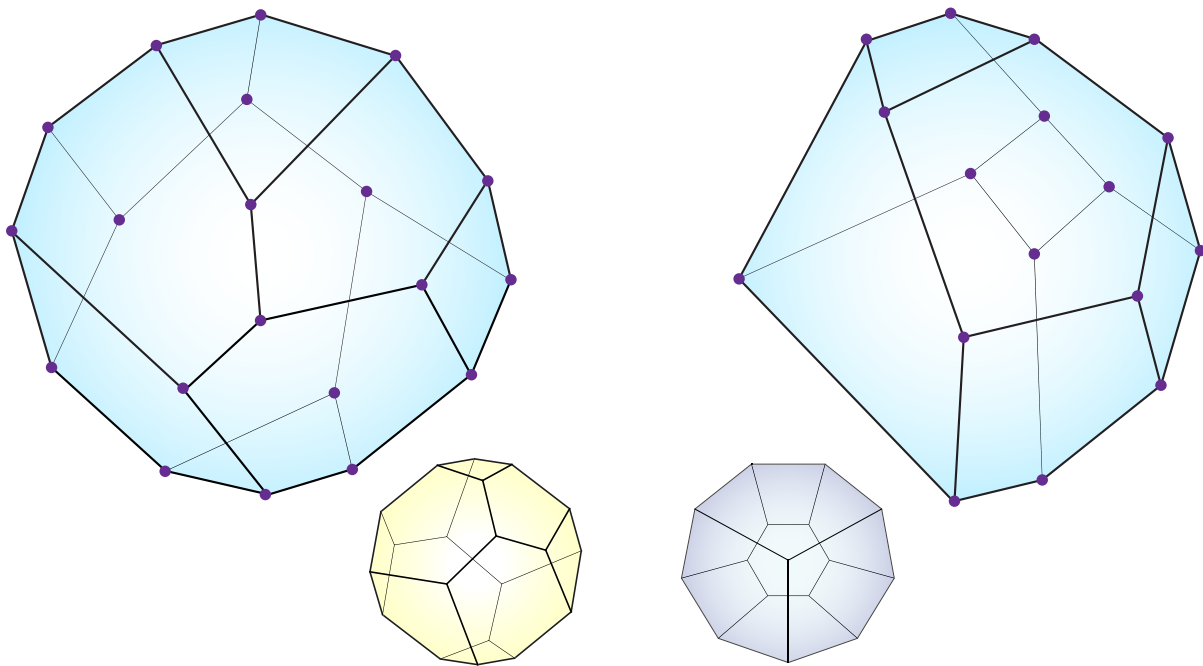


FIGURE 19. On the left is the Hasse diagram for  $n$ -tubings of the cycle graph, with the cyclohedron pictured below for comparison. On the right is the Hasse diagram for  $n$ -tubings of the star graph, with the stellohedron pictured below.

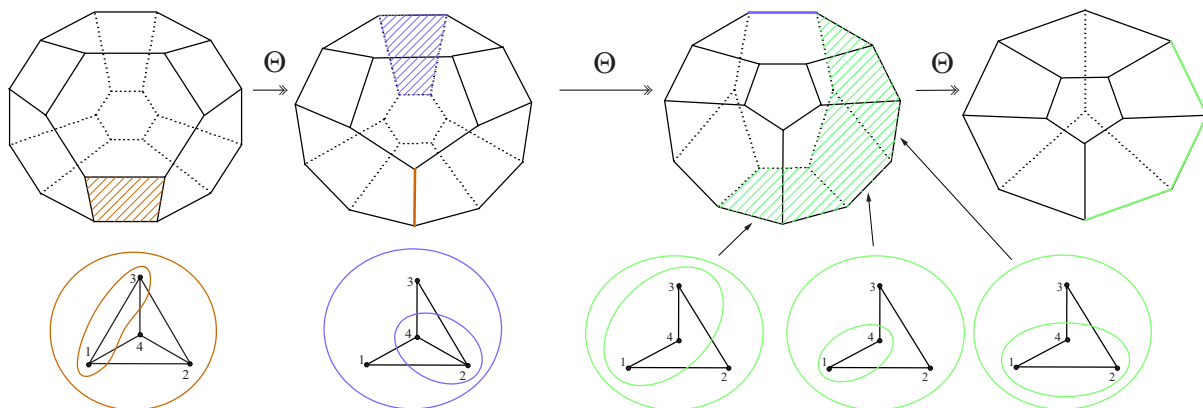


FIGURE 20. A factorization of the Tonks projection through 3 dimensional graph associahedra. The shaded facets correspond to the shown tubings, and are collapsed as indicated to respective edges. The pictured polytopes are  $\mathcal{P}_4, Pt_4, \mathcal{W}_4$  and  $\mathcal{K}_4$  from left to right.

**3.8. Diameters, flips and the Hirsch conjecture.** Is there a polynomial upper bound for the maximum distance between vertices (via a path of edges) for all  $n$ -dimensional polytopes with  $k$ -facets?

The answer to this question is currently unknown. For more than fifty years the question was conjectured to have the answer that the maximum distance, or *graph diameter*, was simply  $k - n$ . This is true for the tetrahedron since  $4 - 3 = 1$ , and all the vertices are only one edge apart. However, in 2010, Francisco Santos found a 43 dimensional polytope with 86 facets, but with two vertices a little further than 43 steps apart. By “found” we mean “showed to exist;” the exact distance is hard to compute when there are likely billions of vertices. This

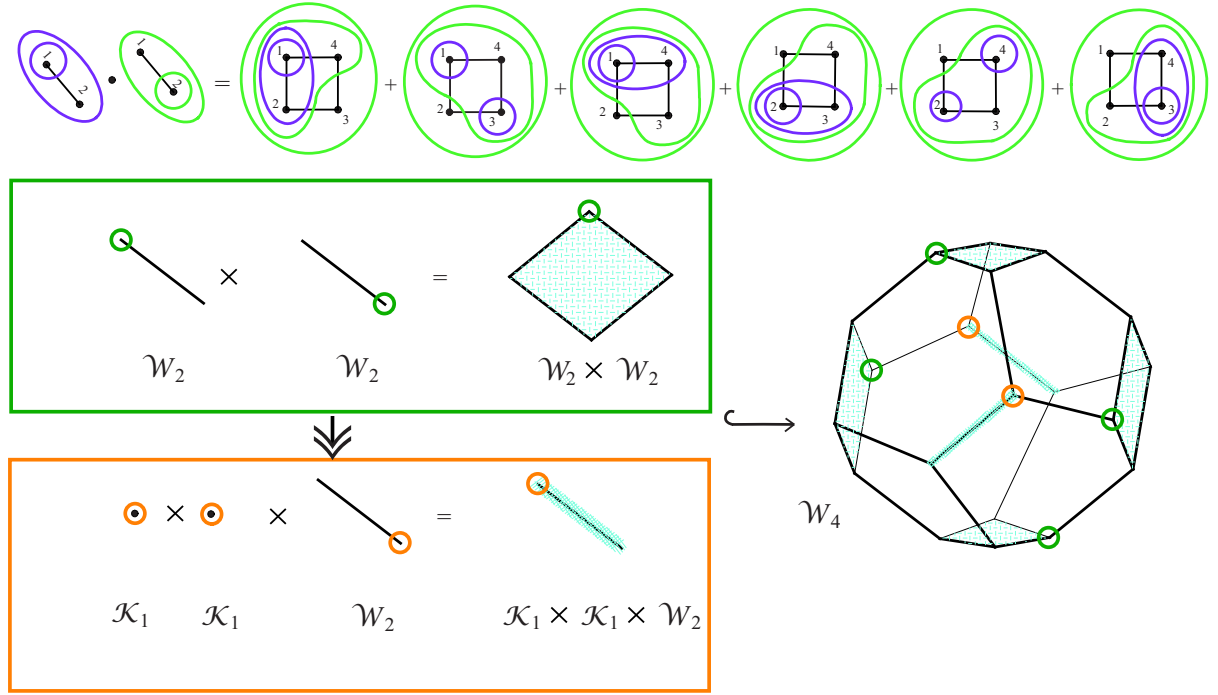


FIGURE 21. As seen in [13], the product of two faces from terms  $\mathcal{W}_i$  and  $\mathcal{W}_j$  of the cyclohedra, is described as a sum of faces of the term  $\mathcal{W}_{i+j}$ . The summed faces in the product are the images of maps which embed cartesian products of earlier terms of  $\{\mathcal{W}_n\}$ , composed with our new extensions of the Tonks projection.

counterexample only increases the interest in answering the question of whether there is a more complicated polynomial in  $k$  and  $n$  that limits the distance between vertices. That the answer is “yes” is known as the polynomial Hirsch conjecture. The Hirsch conjecture and any lower bounds on it are of value to those using linear programming to find optimal design solutions. This is because the diameter of a polytope provides an upper limit for the number of steps in the simplex algorithm—which maximizes a linear functional over that polytope.

Very promising is the fact that our new construction unifies a great deal of existing examples in which the edges of the polytope have combinatorial “flip graph” descriptions. Each edge of a poset associahedron can be interpreted as a flip, where one tube of a tubing is removed and another uniquely determined tube takes its place. (See Figure 22 for an example.) This both unites and generalizes the meaning of edges in associahedra, permutohedra, and graph associahedra. In terms of diameters of these polytopes, it allows a path in the 1-skeleton to be interpreted as a series of flips connecting two combinatorial objects.

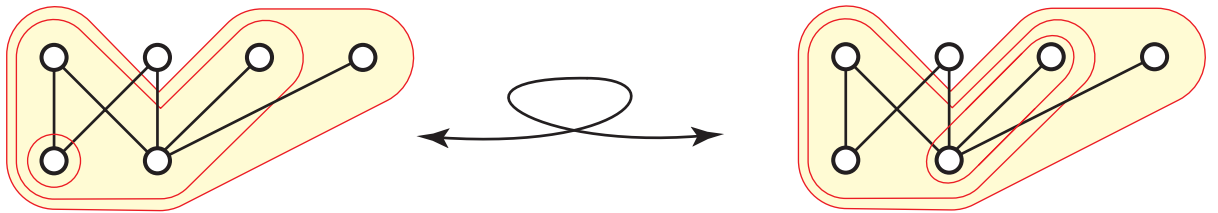


FIGURE 22. Each edge of a poset associahedron can be interpreted as a flip, where one tube is removed and another uniquely determined tube takes its place.

Studying the flip distance between triangulations of a polygon or between binary trees has led to recent success in finding the diameters of associahedra, from Pournin [24]. This success has ignited much interest, including our own, in extending these results to related polytope sequences. Interestingly, the results of Pournin conform to the polynomial Hirsch conjecture for the diameters of polytopes. We hope that by finding new formulas for the diameters of infinite sequences of polytopes we can establish lower bounds (conjecturally polynomial in the dimension and number of vertices) on the polynomial Hirsch conjecture.

**3.9. Convex combinatorics and phylogenetic trees.** Just as finding the etymology of an unfamiliar word can help us discern its meaning, knowledge of the historical development of a gene can be a key to determining its function.

Being able to isolate genes and collections of genes that are related to disorders in an organism is of inestimable value for medicine. Despite our ability to sequence the genome, we are far from knowing even a tiny percentage of what traits are coded for in most of it. Every new method of finding the specific functions a gene corresponds to brings the potential of a new genetic therapy, or a new screening that can catch problems before they are serious.

**3.10. Statistics and combinatorics.** The goal is to start with a set of genomes, the common DNA of a theoretically related set of species (or a set of DNA samples from individuals) and to produce a history. This has been done in several ways, most recently by Pachter and his coauthors. They demonstrate that the so-called neighbor-net algorithm produces from a DNA data a tubing on a path graph. [20, 16, 15]

Recently S. Devadoss and students have developed methods of taking DNA data from a set of species and creating a tubing on a general graph. We plan to collaborate on the application of this method, since the P.I. has found ways to relate a graph tubing to a phylogenetic network.

The final result will be a branching network, with a basic tree-like structure that also has potentially several roots and limbs that may rejoin at a higher, later level. The latter will represent the occurrence of lateral gene transfer, or hybridization.

**3.11. How to start with a face of a graph associahedron and get a phylogenetic tree.** The nodes of a graph are labeled by a collection of species, combinatorially described by their genomes. Edges in the graph represent contribution of DNA, either by descent (mutation) or by hybridization. Tubes in the graph show time progression: a node outside a tube is a direct ancestor of nodes it is adjacent to inside that tube. Thus in complete tubings there is no ambiguity in time progression, but ambiguities may be represented in incomplete tubings.

The following figures show how to interpret a graph tubing as a phylogenetic tree. Figure 23 is a complete tubing—it has 7 nodes and 6 tubes. Figure 24 is incomplete—two tubes have been removed. Thus a single higher face contains inside it the potential of all its finer subfaces.

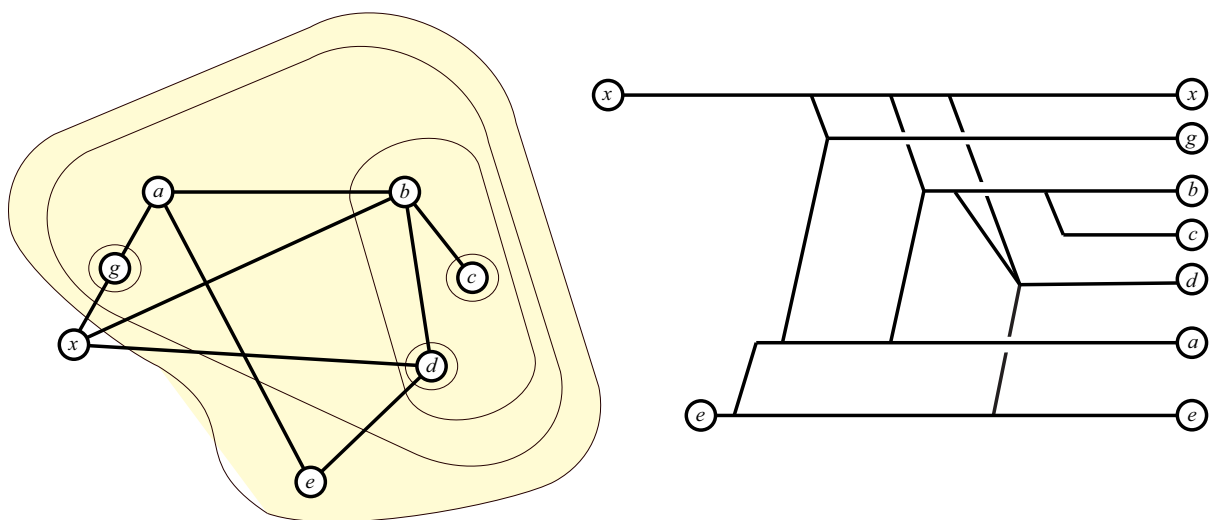


FIGURE 23. Horizontal lines on the right represent genomes, and time progresses to the right.

$g$  is a hybrid of  $x$  and  $a$   
 $b$  is a hybrid of  $x$  and  $a$   
 $c$  is a mutation of  $b$   
 $d$  is a hybrid of  $x$ ,  $b$  and  $e$   
 $a$  is a mutation of  $e$ .

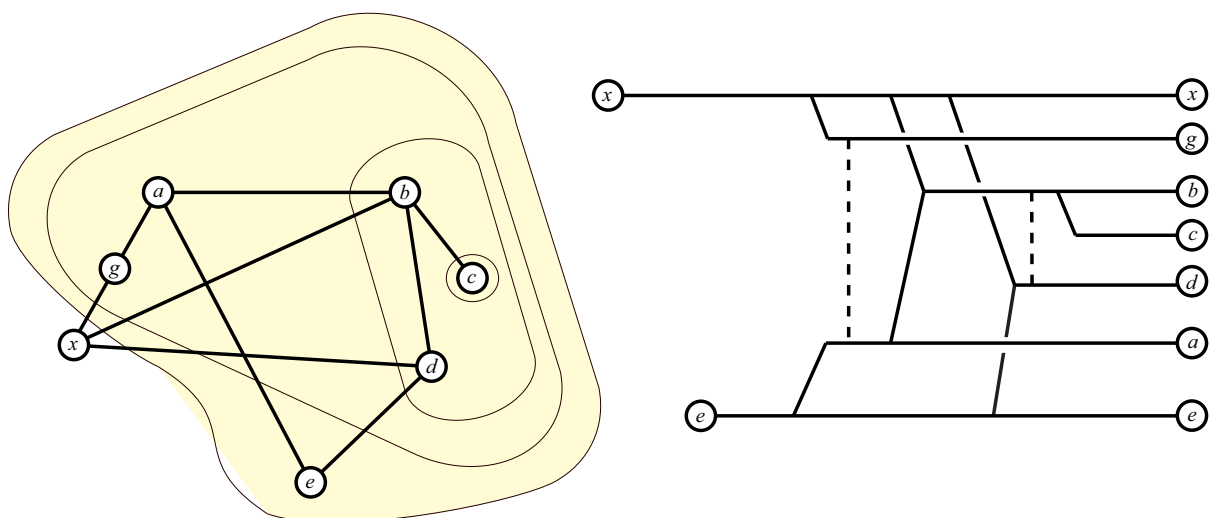


FIGURE 24. In this example some tubes have been removed, allowing ambiguity in time progression. Now we have, for example:  
 Either  $g$  is a hybrid of  $x$  and  $a$ , or  $a$  is a hybrid of  $e$  and  $g$ .

## REFERENCES

- [1] Marcelo Aguiar, N. Bergeron, and Frank Sottile. Combinatorial hopf algebras and generalized dehn-somerville relations. *Compos. Math.*
- [2] Marcelo Aguiar and Frank Sottile. Structure of the Malvenuto-Reutenauer Hopf algebra of permutations. *Adv. Math.*, 191(2):225–275, 2005.
- [3] Marcelo Aguiar and Frank Sottile. Structure of the Loday-Ronco Hopf algebra of trees. *J. Algebra*, 295(2):473–511, 2006.
- [4] Federico Ardila and Jeffrey Doker. Lifted generalized permutahedra and composition polynomials. *preprint*, <http://arxiv.org/abs/1201.2977>, 2012.
- [5] Michael Carr, Satyan Devadoss, and Stefan Forcey. Pseudograph associahedra. *Journal of Combinatorial Theory, Series A*, 118(7):2035–2055, 2009.
- [6] Michael P. Carr and Satyan L. Devadoss. Coxeter complexes and graph-associahedra. *Topology Appl.*, 153(12):2155–2168, 2006.
- [7] Frédéric Chapoton. Bigèbres différentielles graduées associées aux permutoèdres, associaèdres et hypercubes. *Ann. Inst. Fourier (Grenoble)*, 50(4):1127–1153, 2000.
- [8] Satyan Devadoss and Stefan Forcey. Marked tubes and the graph multiplihedron. *Algebr. Geom. Topol.*, 8(4):2081–2108, 2008.
- [9] Satyan L. Devadoss. A realization of graph associahedra. *Discrete Math.*, 309(1):271–276, 2009.
- [10] Satyan L. Devadoss, T. Heath, and C. Vipismakul. Deformations of bordered surfaces and convex polytopes. *Notices of the A. M. S.*, 58(1):530–541, 2011.
- [11] Stefan Forcey. Convex hull realizations of the multiplihedra. *Topology Appl.*, 156(2):326–347, 2008.
- [12] Stefan Forcey, Aaron Lauve, and Frank Sottile. Cofree compositions of coalgebras (extended abstract). *DMTCS Proc. FPSAC 22*, pages 363–374, 2011.
- [13] Stefan Forcey and Derriell Springfield. Geometric combinatorial algebras: cyclohedron and simplex. *preprint*.
- [14] Florent Hivert, Jean-Christophe Novelli, and Jean-Yves Thibon. Commutative combinatorial Hopf algebras. *J. Algebraic Combin.*, 28(1):65–95, 2008.
- [15] Daniel. Huson and Celine Scornavacca. A survey of combinatorial methods for phylogenetic networks. *Genome Biol Evol.*, 3:23–35, 2011.
- [16] D. Levy and Lior Pachter. The neighbor-net algorithm. *Advances in Applied Mathematics*, 47:240–258, 2011.
- [17] Jean-Louis Loday and María O. Ronco. Combinatorial hopf algebras. *arxiv preprint*.
- [18] Jean-Louis Loday and María O. Ronco. Hopf algebra of the planar binary trees. *Adv. Math.*, 139(2):293–309, 1998.
- [19] Claudia Malvenuto and Christophe Reutenauer. Duality between quasi-symmetric functions and the Solomon descent algebra. *J. Algebra*, 177(3):967–982, 1995.
- [20] Lior Pachter and Bernd Sturmfels. The mathematics of phylogenomics. *SIAM review*, 49:3–31, 2007.
- [21] V. Pilaud and Santos F. The brick polytope of a sorting network. *European J. Combin.*, to appear, 2012.
- [22] Alex Postnikov, Victor Reiner, and Lauren Williams. Faces of generalized permutohedra. *Doc. Math.*, 13:207–273, 2008.
- [23] Alexander Postnikov. Permutohedra, associahedra, and beyond. *Int. Math. Res. Not. IMRN*, (6):1026–1106, 2009.
- [24] Lionel Pournin. The diameters of associahedra. *preprint*, <http://arxiv.org/pdf/1207.6296v2.pdf>, 2012.
- [25] Nathan Reading. From the tamari lattice to cambrian lattices and beyond. In J. Marcel J. Stasheff F. Mller-Hoissen, J. Pallo, editor, *Associahedra, Tamari Lattices and Related Structures: Tamari Memorial Festschrift*, volume 299 of *Progress in Mathematics*, pages 299–322. 2012.
- [26] Maria Ronco. Generalized tamari order. In J. Marcel J. Stasheff F. Mller-Hoissen, J. Pallo, editor, *Associahedra, Tamari Lattices and Related Structures: Tamari Memorial Festschrift*, volume 299 of *Progress in Mathematics*, pages 339–350. 2012.
- [27] Samson Sanedlidze and Ronald Umble. Matrads, biassociahedra, and  $a_\infty$ -bialgebras. *Homology Homotopy Appl.*, 13(1):1–57 (electronic), 2011.
- [28] T. Tradler. Infinity inner products on a-infinity algebras. *Journal of Homotopy and Related Structures*, 3(1):245–271, 2008.
- [29] Andrei Zelevinsky. Nested complexes and their polyhedral realizations. *Pure Appl. Math. Q.*, 2(3, part 1):655–671, 2006.